Research Article

54

INDONESIAN SCHOLAR SOCIETY

Indones. J. Chem. Stud.
2023, 2(2), 54–60
Available online at journal.solusiriset.com
e-ISSN: 2830-7658; p-ISSN: 2830-778X

Indonesian Journal of Chemical Studies

Comparative Analysis of Electronic Structures Calculations: A Simple Test Case Set for Kohn-Sham Density Functional Theory and Hartree-Fock Methods

Yusuf Bramastya Apriliyanto[1]*, Naufan Nurrosyid[2]

[1]*Department of Chemistry, Republic of Indonesia Defense University, Kawasan IPSC Sentul, Bogor 16810, Indonesia*

[2]*Department of Materials Science & Engineering, Monash University, 20 Research Way, Clayton VIC 3800, Australia*

Received: 02 Sep 2023; Revised: 26 Oct 2023; Accepted: 27 Oct 2023;
Published online: 10 Nov 2023; Published regularly: 31 Dec 2023

Abstract—A comparative analysis on the performance of Kohn-Sham density functional theory (KS-DFT) and Hartree-Fock (HF) methods to obtain reliable energy and electronic properties has been performed in this study using a simple test case. It is crucial to re-emphasize the key differences between these methods to address common conceptual difficulties that occur among freshmen studying basic computational chemistry. The results suggested that the eigenvalue theorem in determining ionization potential could be well implemented in the HF but not in the KS-DFT method. The total energy difference between ionized and non-ionized species was an appropriate procedure to calculate the first ionization potential within the KS-DFT method. The HOMO-LUMO gap in the HF was larger than the gaps obtained from the KS-DFT method. Among all of the performed calculation methods, the B3LYP hybrid functional provided better total energy where the eigenvalues were located between the HF and the LDA/GGA functionals.

Keywords— *Hartree-Fock; DFT; Electronic structures; Orbitals.*

1. INTRODUCTION

In the field of computational materials science (*e.g.* computational physics and computational chemistry), density functional theory (DFT) has emerged as the most popular numerical method used to determine different properties of atoms, molecules, supramolecules, and solids in the last few decades [1,2]. The DFT-related literature has grown exponentially during the 1990s, whereas since 2000, the growth has become linear. Nowadays, the DFT publication volume is estimated to double every 5–6 years [3]. Among high-level first-principles calculation methods, the development of DFT has had a considerable impact on molecular calculations. It is now feasible and possible to obtain results close to chemical accuracy (an accuracy of 1 kcal mol^{-1}) for systems composed of several hundred atoms. DFT provides insight into energetical, structural, chemical reaction mechanisms, spectroscopic features, as well as force fields parameterization of classical molecular simulations [4–8].

The development of DFT is based on quantum mechanics. Quantum mechanics reveal that all the information we want to know about a system is contained in a certain function. For a system comprising N electrons, this function depends on one spin (1N) and three spatial coordinates (3N) for every electron at a fixed nuclear position. This complicated function which in total depends on 4N variables, is known as the wave function. Following basic quantum mechanics, a given external potential (the potential of nuclear charges, $V(r)$) and a given number of electron N, all of those forms the Hamiltonian operator ($\hat{H}$), determine the ground state wave function and thus the corresponding electron density (except for degeneracies). The ground state electron density is the square of its ground state wave function. By integrating spin into it, it produces spin density that only depends on 3 spatial coordinates, $\rho(x, y, z)$ [9].

Unlike the wave function, electron density (ρ) is a function that is independent of the total electrons in a given system (only 3 variables rather than 3N). As a result, it is not largely affected by the system size. While a wave function method complexity escalates exponentially with the total of electrons, by simplifying

***Corresponding author**.
Email address: yusuf.bramastya@gmail.com
DOI: 10.55749/ijcs.v2i2.33

the problem through electron density (ρ), we can speed up the energy calculation of a system. This method is known as the Density Functional Theory (DFT). However, there is no prescription for how to select the candidate densities rationally. The first theoretical approach to describe atoms using electron density instead of wave function is the Thomas-Fermi model. It is formulated using the concept of non-interacting uniform electron gas, in which the total energy is calculated as a sum (integral) over volume elements so that the electron density in each element is considered to be uniform. This is known as the Local Density Approximation (LDA) in modern DFT [10].

Kohn and Sham in 1965 proposed a practical computational scheme by replacing energy minimization concerning one unknown function ρ (the density) with a minimization for several unknown functions φ_i (the occupied orbitals). In the Kohn-Sham formalism, the kinetic part ($T[\rho]$) is split into two components, one that can be calculated exactly and a small correction term. The latter then will be lumped together with the $V_{ee}[\rho] - J[\rho]$ terms as a single term called the exchange-correlation energy, E_{xc}. The consequence is that orbitals are reappeared; thus bringing back the complexity from 3 to 3N variables (as the wave function method) and electron exchange-correlation terms reemerge as a separate component. The Kohn-Sham (KS) method is closely resembles the Hartree-Fock (HF) wave function method, sharing identical formulas for the Coulomb electron–electron, electron–nuclear, and kinetic energies [9,11]. It is known that HF self-consistent field approximation is the starting point for most *ab initio* or wave function based methods.

In order to perform Kohn-Sham DFT (KS-DFT), all we need to know is the $E_{xc}[\rho(r)]$. The exact analytical expressions for this functional are not known. Therefore, some approximations are required. Many approximations have been invented to provide exchange-correlation functionals, starting from LDA, Local Spin Density Approximation (LSDA), Generalized Gradient Approximation (GGA) and meta-GGA, up to hybrid DFT functionals [12]. Up to this stage, students studying basic computational chemistry are often confused about the advantages and disadvantages of the KS-DFT than the HF methods because they are pretty similar in their formulation of orbitals and their system size dependency; despite their scaling factor in terms of computational cost and the produced electronic properties are different [9-11].

Therefore, it is noteworthy to re-emphasize the key differences among HF and KS-DFT methods in determining the electronic properties of atoms, ions, and molecules. In this paper, a simple comparative performance analysis of the HF and KS-DFT methods is evaluated to address common conceptual difficulties that occur among freshmen studying basic computational chemistry.

2. METHODS

In our calculations, we investigated some simple systems ranging from atoms, ions, and an organic molecule (imidazole). Three types of Dunning's correlation-consistent polarized (cc-p) basis sets of split valence double-zeta, triple-zeta, and quadruple-zeta (cc-pVDZ, cc-pVTZ, and cc-pVQZ) were employed in our HF and KS-DFT calculations. In order to be able to treat ions or systems with more spatially diffused molecular orbitals, diffuse functions were introduced into each of the above basis sets, forming the aug-cc-pVDZ, aug-cc-PVTZ, and aug-cc-pVQZ. For the KS-DFT method, different exchange and correlation functionals were implemented, namely the LDA, GGA (PBE), and hybrid DFT (B3LYP). The molecular geometries of imidazole were optimized at the corresponding calculation methods and checked the vibrational frequencies to obtain the most stable structures. We analyzed the obtained HF and KS-DFT total energies and their convergence with respect to basis sets. Furthermore, their molecular orbitals were also investigated, emphasizing the HOMO, LUMO, and their energy gap along with their ionization energies. All of the performed calculations were conducted using a quantum chemistry program, Orca [13]. Meanwhile, molecular structure and its orbitals were visualized using the Jmol computer application [14].

3. RESULT AND DISCUSSION

3.1. Theoretical Background

HF and KS-DFT have in common aspect that both produce a set of self-consistent orbitals with a set of eigenvalues, representing the orbitals' energies. To differentiate both methods, first, students have to examine the theoretical background behind their formulation. Similar to the wave function method, the set of eigenfunctions and eigenvalues in KS-DFT is obtained by providing initial guess functions φ_i and then refined following the self-consistent procedure (Eq. 1).

$$h_i^{KS}\,\varphi_i = \varepsilon_i\,\varphi_i \tag{1}$$

The Kohn-Sham (KS) one-electron operator, h_i^{KS}, is defined as

$$h_i^{KS} = -\frac{1}{2}\nabla_i^2 - \sum_{k=1}^{nuclei}\frac{Z_k}{|r_i - r_k|} + \int\frac{\rho(r')}{|r_i - r'|}\,dr' + V_{xc}[\rho(r)] \tag{2}$$

Where r indicates spatial coordinates and $V_{xc}[\rho(r)]$ is a functional derivative given by

$$V_{xc}[\rho(r)] = \frac{\delta E_{xc}[\rho(r)]}{\delta\rho(r)} \tag{3}$$

The last three terms in Eq. 2 as a unity is called the Kohn-Sham effective potential (V_{eff}^{KS}), while the eigenvectors $\{\varphi_i\}$ and the eigenvalues $\{\varepsilon_i\}$ are called the Kohn-Sham orbitals and the Kohn-Sham orbital energies [9,10].

The eigenvalues $\{\varepsilon_i\}$ do not have a simple physical interpretation, except for the highest one (HOMO). The relationship between ε_{max} and the ionization potential (I) follows Janak's theorem, for the exact exchange-correlation potential, defined by

$$I = E_N - E_{N+1} = -\varepsilon_{max} \quad (4)$$

However, the sum of the eigenvalues $\{\varepsilon_i\}$ cannot simply be related to the total energy. The total energy is calculated from the following formula (Eq. 5) using the best density obtained after the self-consistent procedure.

$$E[\rho(r)] = T_s[\rho(r)] + V_{ne}[\rho(r)] + J[\rho(r)] + E_{xc}[\rho(r)] \quad (5)$$

The self-consistent procedure to solve the KS equations resembles closely the one in HF. The difference is in the use of effective potential. In the KS effective potential (V_{eff}^{KS}), the HF exchange integrals are replaced with the $V_{xc}[\rho(r)]$ term. In addition, the KS effective potential includes also the electron correlation in the $V_{xc}[\rho(r)]$ term, while in the HF the electron correlation is neglected. With all of the aforementioned formulations, KS-DFT scales as N^3 (except for hybrid DFT), while HF scales as N^4 (N is the total electrons). These aspects are among the advantages of using KS-DFT, at a relatively lower computational cost, providing more accurate energetical results than the HF [1,11]. In the next section, some simple calculations involving atoms, ions, and a small organic molecule are discussed as a further analysis of the HF and KS-DFT methods.

Table 1. The results of the Kohn-Sham DFT calculations using LDA approximation

Atoms/ Ions	Basis sets	Total Energy (eV)	HOMO (eV)	LUMO (eV)	E_{Gap} (eV)	$I = -\varepsilon_{max}$ (eV)	I = (N-1)-N (eV)
He	cc-pVDZ	-76.91869	-15.14330	29.58250	44.72580	15.14330	24.22452
	aug-cc-pVDZ	-76.98595	-15.49800	2.69660	18.19460	15.49800	24.28125
	cc-pVTZ	-77.11924	-15.46560	12.42360	27.88920	15.46560	24.30095
	aug-cc-pVTZ	-77.12666	-15.51840	1.66130	17.17970	15.51840	24.30829
	cc-pVQZ	-77.13248	-15.49580	9.47870	24.97450	15.49580	24.30045
	aug-cc-pVQZ	-77.13590	-15.52230	1.48520	17.00750	15.52230	24.30380
Li	cc-pVDZ	-199.76795	-3.17190	-2.12420	1.04770	3.17190	5.45003
	aug-cc-pVDZ	-199.76882	-3.17250	-2.12990	1.04260	3.17250	5.45038
	cc-pVTZ	-199.81891	-3.16060	-2.09190	1.06870	3.16060	5.46714
	aug-cc-pVTZ	-199.81972	-3.16290	-2.10020	1.06270	3.16290	5.46762
	cc-pVQZ	-199.82454	-3.16300	-2.09800	1.06500	3.16300	5.47012
	aug-cc-pVQZ	-199.82489	-3.16350	-2.09840	1.06510	3.16350	5.47030
Li^+	cc-pVDZ	-194.31792	-59.08610	-6.43210	52.65400	59.08610	75.54817
	aug-cc-pVDZ	-194.31844	-59.08790	-6.43180	52.65610	59.08790	75.54863
	cc-pVTZ	-194.35177	-59.52650	-6.50190	53.02460	59.52650	74.57650
	aug-cc-pVTZ	-194.35210	-59.52830	-6.50290	53.02540	59.52830	74.57682
	cc-pVQZ	-194.35442	-59.54480	-6.53150	53.01330	59.54480	74.58037
	aug-cc-pVQZ	-194.35459	-59.54560	-6.53120	53.01440	59.54560	74.58050
Be	cc-pVDZ	-393.02859	-5.60970	-2.06410	3.54560	5.60970	9.05800
	aug-cc-pVDZ	-393.03152	-5.61920	-2.09030	3.52890	5.61920	9.05366
	cc-pVTZ	-393.10304	-5.60170	-2.08900	3.51270	5.60170	9.02263
	aug-cc-pVTZ	-393.10490	-5.60100	-2.09360	3.50740	5.60100	9.02288
	cc-pVQZ	-393.10952	-5.59630	-2.09220	3.50410	5.59630	9.02435
	aug-cc-pVQZ	-393.11019	-5.59770	-2.09650	3.50120	5.59770	9.02449
Ne	cc-pVDZ	-3487.30657	-12.21780	35.10010	47.31790	12.21780	21.84041
	aug-cc-pVDZ	-3487.88188	-13.59660	3.50120	17.09780	13.59660	22.28207
	cc-pVTZ	-3488.87068	-13.12880	21.97040	35.09920	13.12880	22.08871
	aug-cc-pVTZ	-3489.00194	-13.57470	2.92730	16.50200	13.57470	22.21178
	cc-pVQZ	-3489.24982	-13.37420	15.71260	29.08680	13.37420	22.14854
	aug-cc-pVQZ	-3489.29453	-13.55970	2.44920	16.00890	13.55970	22.18982
Ar	cc-pVDZ	-14310.80449	-10.12660	14.57380	24.70040	10.12660	16.09741
	aug-cc-pVDZ	-14310.90211	-10.41320	1.12330	11.53650	10.41320	16.18202
	cc-pVTZ	-14311.36724	-10.34350	9.67490	20.01840	10.34350	15.99497
	aug-cc-pVTZ	-14311.38288	-10.41770	0.97390	11.39160	10.41770	16.26417
	cc-pVQZ	-14311.49728	-10.38400	6.48030	16.86430	10.38400	16.25974
	aug-cc-pVQZ	-14311.50198	-10.40750	0.67110	11.07860	10.40750	16.26370

Table 2. The results of the Kohn-Sham DFT calculations using GGA (PBE) approximation

Atoms/ Ions	Basis sets	Total Energy (eV)	HOMO (eV)	LUMO (eV)	E_{Gap} (eV)	$I = -\varepsilon_{max}$ (eV)	I = (N-1)-N (eV)
He	cc-pVDZ	-78.49029	-15.37890	29.19430	44.57320	15.37890	24.37771
	aug-cc-pVDZ	-78.55927	-15.72860	2.48180	18.21040	15.72860	24.43980
	cc-pVTZ	-78.69911	-15.70290	12.24740	27.95030	15.70290	24.46429
	aug-cc-pVTZ	-78.70705	-15.75790	1.49080	17.24870	15.75790	24.47211
	cc-pVQZ	-78.71313	-15.73480	9.26250	24.99730	15.73480	24.46441
	aug-cc-pVQZ	-78.71668	-15.76260	1.32720	17.08980	15.76260	24.46780
Li	cc-pVDZ	-203.00777	-3.24430	-0.66480	2.57950	3.24430	5.57545
	aug-cc-pVDZ	-203.00903	-3.24620	-0.65620	2.59000	3.24620	5.57579
	cc-pVTZ	-203.02253	-3.22090	-0.53470	2.68620	3.22090	5.58249
	aug-cc-pVTZ	-203.02372	-3.22440	-0.54730	2.67710	3.22440	5.58311
	cc-pVQZ	-203.02815	-3.22330	-0.39360	2.82970	3.22330	5.58389
	aug-cc-pVQZ	-203.02875	-3.22480	-0.32250	2.90230	3.22480	5.58414
Li^+	cc-pVDZ	-197.43232	-60.26910	-6.62660	53.64250	60.26910	76.58952
	aug-cc-pVDZ	-197.43324	-60.27160	-6.62670	53.64490	60.27160	76.59043
	cc-pVTZ	-197.44004	-60.31570	-6.76240	53.55330	60.31570	75.34824
	aug-cc-pVTZ	-197.44061	-60.31800	-6.75930	53.55870	60.31800	75.34869
	cc-pVQZ	-197.44426	-60.33970	-6.80500	53.53470	60.33970	75.35566
	aug-cc-pVQZ	-197.44461	-60.34090	-6.80460	53.53630	60.34090	75.35585
Be	cc-pVDZ	-398.03711	-5.63620	-1.99360	3.64260	5.63620	9.04283
	aug-cc-pVDZ	-398.03962	-5.64320	-2.01900	3.62420	5.64320	9.03936
	cc-pVTZ	-398.06600	-5.61290	-2.00510	3.60780	5.61290	8.99469
	aug-cc-pVTZ	-398.06604	-5.61280	-2.01240	3.60040	5.61280	8.99461
	cc-pVQZ	-398.07418	-5.60750	-2.01110	3.59640	5.60750	8.99671
	aug-cc-pVQZ	-398.07530	-5.61090	-2.01810	3.59280	5.61090	8.99722
Ne	cc-pVDZ	-3504.63749	-12.02700	35.63420	47.66120	12.02700	21.20031
	aug-cc-pVDZ	-3505.21382	-13.40440	3.43100	16.83540	13.40440	21.75899
	cc-pVTZ	-3506.07611	-12.87750	22.32040	35.19790	12.87750	21.53394
	aug-cc-pVTZ	-3506.22546	-13.35940	2.84770	16.20710	13.35940	21.67867
	cc-pVQZ	-3506.46811	-13.13930	15.91310	29.05240	13.13930	21.60772
	aug-cc-pVQZ	-3506.52387	-13.35230	2.32170	15.67400	13.35230	21.66102
Ar	cc-pVDZ	-14349.10571	-10.03400	14.95190	24.98590	10.03400	15.70449
	aug-cc-pVDZ	-14349.19524	-10.30700	1.18260	11.48960	10.30700	15.78117
	cc-pVTZ	-14349.56654	-10.20310	9.91400	20.11710	10.20310	15.70184
	aug-cc-pVTZ	-14349.58867	-10.29500	1.00700	11.30200	10.29500	15.71664
	cc-pVQZ	-14349.68171	-10.25860	6.58070	16.83930	10.25860	15.70101
	aug-cc-pVQZ	-14349.68856	-10.29020	0.64450	10.93470	10.29020	15.70666

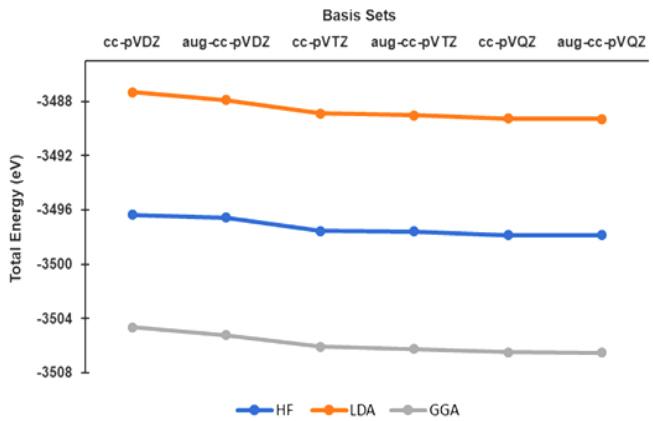

Fig. 1 Energy convergence as a function of basis sets size for Ne atom calculated using the KS-DFT and HF methods

3.2. Atoms / Ions

Among KS-DFT methods, two basic approximations commonly used for estimating $V_{xc}[\rho(r)]$ functionals are LDA and GGA (here, we selected the PBE functional) [2]. These exchange-correlation functionals have been employed in our calculation to compute the energy of various systems involving atoms/ions by using different basis sets (**Table 1** and **Table 2**). Based on the results presented in **Table 1** and **Table 2**, the total energy of each atom/ion with respect to the size of the basis set is monotonic, having a similar value. Large basis sets, indeed, provide lower energy (variational principle), but the energy does not change much (already converged). The energy convergence with respect to the basis set size can also be seen in **Fig. 1**. Unlike the wave function theory, the DFT enjoys a much faster basis set convergence.

The convergence of the orbital eigenvalues at the frontier orbitals (*i.e.* HOMO and LUMO) and their energy gap with the size of the basis sets were also investigated. The eigenvalues for HOMO and LUMO, and the gap between HOMO and LUMO were fluctuate with

respect to the size of the basis sets (**Table 1** and **Table 2**). They did not converge to lower values. These phenomena were further investigated by computing the first ionization potentials (I) in comparison with the experimental ionization potential values [15]. The KS-DFT first ionization potentials (reported in **Table 1** and **Table 2**) were calculated following the eigenvalue theorem (Janak's theorem) as the negative of HOMO (ε_{max}). The ionization potentials obtained from the calculations were very different from the experimental values reported in **Table 3** [15]. This problem arises from the fact that the obtained eigenvalues (in this case the HOMO) are not accurate. There are still some errors in the functionals used for the calculations, such as the self-interaction error, that lead to incorrect position of the eigenvalues (HOMO, LUMO, etc.) and incorrect values of the gap. The self-interaction error makes the electron repulsions too large; thus, the occupied orbital energies are shifted up (as does the HOMO, which leads to smaller ionization potentials). Therefore, the eigenvalue theorem is not applicable in this case. As we know, the eigenvalue theorem is valid only for the exact exchange-correlation potential implemented in DFT.

Table 3. The first ionization potentials for various atoms/ions

Atoms/ ions	First Ionization Potentials	
	HF, aug-cc-pVQZ (eV)	Experimental (eV) [15]
He	24.97820	24.5874
Li	5.34340	5.3917
Li^+	75.98390	75.6400
Be	8.41570	9.3227
Ne	23.14750	21.5645
Ar	16.08400	15.7596

A similar eigenvalue theorem as Janak's theorem in DFT also exists in the HF wave function method (*i.e.* Koopman's theorem). Koopman's theorem states that the negative of the HOMO eigenvalue from Hartree-Fock calculations can be used to estimate the first ionization potentials. In fact, the Janak's theorem is an analogous of the Koopman's theorem which has been developed earlier. **Table 3** shows that the ionization potentials of the HF method calculated using Koopman's theorem are similar to the experimental values. These results are better than the ionization potentials from the eigenvalue theorem of KS-DFT for both LDA and GGA (**Table 1** and **Table 2**). There is no self-interaction error in the HF method. Thus, it yields better results.

For the case of the KS-DFT method, we also performed additional calculations for the ionized species of all atoms/ions considered in this study and evaluated the ionization potential as the difference of total energies in N and N-1 electrons. The results are presented in the last columns of **Table 1** and **Table 2**. The ionization potentials obtained by subtracting the total energy of the ionized species from the initial species have similar values with the HF and experimental data (**Table 3**). This procedure yields better ionization potentials than using the eigenvalue theorem ($I = -\varepsilon_{max}$). This phenomenon is due to the fact that the DFT is designed to calculate the total energy from the density by continuously selecting and evaluating different densities (variational principle). As a result, computing the ionization potentials from the total energy difference of the two species is a very appropriate procedure.

However, the LDA and PBE calculations using the total energy difference procedure (I = (N-1)-N) produced ionization potentials much more closer to the experimental values than the HF. Since in the HF method the electron correlation is neglected, more errors will occur in systems with more electrons (Ne and Ar). On the other hand, the DFT method has no problem as long as the functional is accurate. In general, among KS-DFT methods, the PBE functional (**Table 2**) produced better results than the LDA (**Table 1**). It generated lower total energy than the LDA and provided ionization potentials (I = (N-1)-N) closer to the corresponding experimental values. PBE is a type of GGA functional that is more physically consistent than LDA. Indeed, the true $V_{xc}[\rho(r)]$ functional of DFT should depend on the density gradient instead of a non-realistic system having a uniform density derived from the uniform electron gas model [12].

3.3. MOs of Organic Molecule

We also performed a further comparative analysis between KS-DFT (LDA, PBE, and B3LYP) and HF methods by investigating the molecular orbitals (MOs) and the energy level diagram of imidazole. The energy level diagram (from HOMO-10 to LUMO+2) and the shape of frontier orbitals (the HOMO and LUMO, depicted in top and side views) are presented in **Fig. 2**. It is important to highlight the fact that the molecular structures in the KS-DFT and HF geometry optimizations are very similar. Moreover, the energy of KS-DFT orbitals depends strongly on the exchange-correlation functional even though the HOMO-LUMO gap remains constant except for the hybrid DFT functional (B3LYP).

In general, the energy gap between HOMO and LUMO in the HF is larger than the gaps obtained from the DFT. Moreover, the occupied orbitals obtained from the DFT have higher energies than the same orbitals obtained from the HF. The occupied orbital energies computed using the LDA and GGA functionals are shifted upward due to the excess of electron repulsion generated from the functionals incompleteness (self-interaction error). However, the B3LYP hybrid functional provides better total energy; and the eigenvalues are located between the HF and the LDA/GGA functionals. This is the result of incorporating some portions of the exact exchange term into B3LYP formulation. B3LYP is the most popular functional in the hybrid DFT method category. Hybrid DFT is a breakthrough; it provides better performance

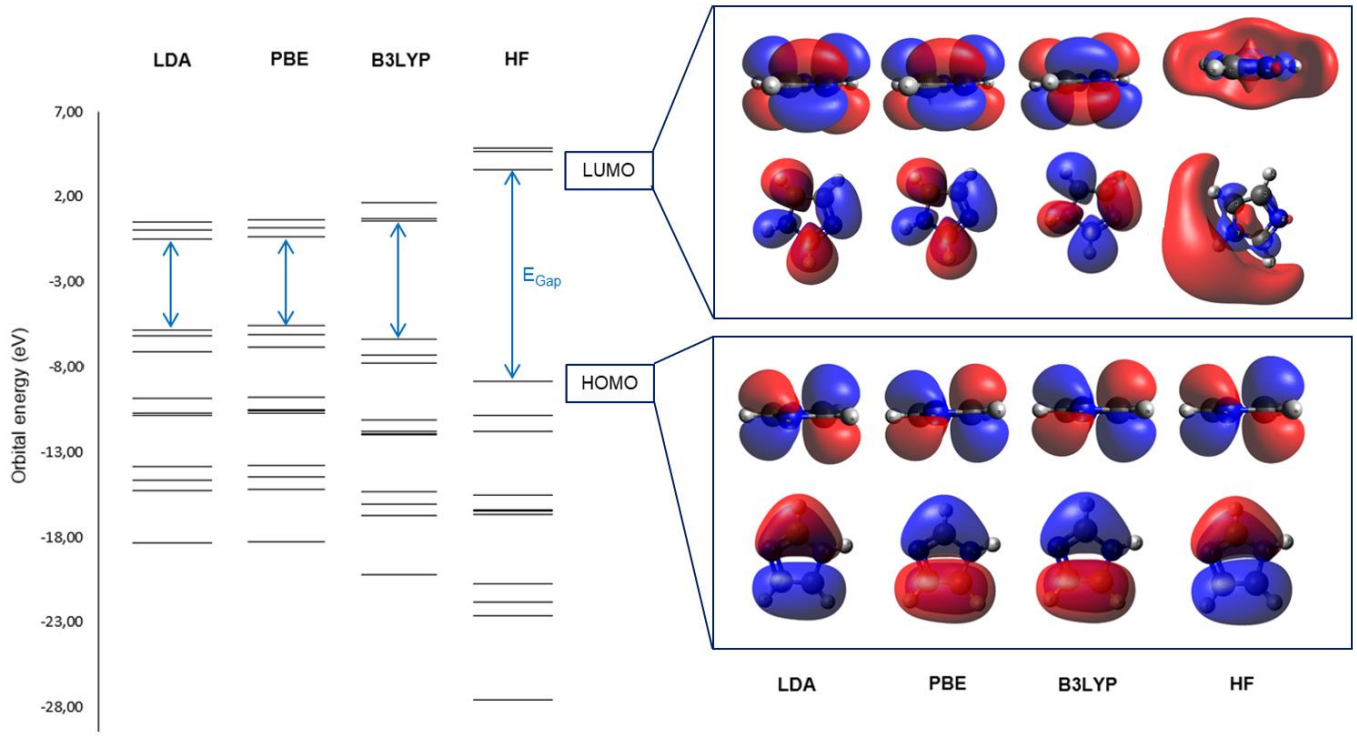

Fig. 2 The energy level diagram and the frontier orbitals computed using various methods for imidazole. The MO energies from HOMO-10 to LUMO+2 are reported for each method

than the standard LDA and GGA functionals. A proper inclusion of exact HF exchange is found to improve the computational outputs, although the optimal fraction of exact HF exchange to include depends on the specific properties of interest [9,10].

Fig. 2 also shows that in general, the HOMO orbitals for all methods have similar shapes, yet the HOMO generated from the HF has a slightly more diffuse shape. On the other hand, all the DFT functionals used in the calculation produced similar LUMO orbitals, but the HF produced a completely different shape. The different shapes should correspond to the LUMO energy. The obtained HF LUMO energy had a high positive value (3.5418 eV), whereas the LDA and PBE had negative values (-0.4968 and -0.3578 eV). The B3LYP functional produced positive LUMO energy (0.5636 eV); however, it is still close to the other DFT results. As the result, the LUMO obtained from B3LYP still had a similar shape to the other DFT results. Based on the definition of methods and their formulations, the unoccupied (virtual) orbitals in HF had different physical meanings and different orbital energies than the KS-DFT counterpart. The unoccupied (virtual) orbitals in HF represent interactions appropriate to a total of N+1 electrons (adding electron), while the unoccupied orbitals in KS-DFT represent a system with N electrons (exciting electron). This is the reason that makes HF unoccupied (virtual) orbitals to be not optimal, having higher energy and a more diffuse shape than KS-DFT virtual orbitals.

It has to be noted that the colors of MOs presented in **Fig. 2** indicate the phase within a system. If their colors are different, then they have different phases. However, for different systems, it is no matter whether the negative and positive phases are in red and blue respectively, or vice versa, or even using different color combinations because they are interchangeable. As an example, in **Fig. 2**, although the LDA and PBE MOs have different colors, they are not distinct orbitals.

Finally, it is worth to highlighting the source of difference between KS-DFT and HF, that is how they treat electron correlation and electron exchange interaction. In DFT, they are treated using an exchange-correlation functional, while in HF, it is measured using the exchange operator and ignores the electron correlation. Additionally, DFT only considers the electron density, whereas HF considers the wave function of each electron individually. The energy function in DFT depends on the density of the electrons, whereas the HF equation depends on the total wave function, a product of each electron wave function represented by a single Slater determinant.

CONCLUSION

As a summary, we performed HF and KS-DFT calculations on atoms, ions, and an organic molecule as a simple test case to re-emphasize the key differences between HF and KS-DFT methods in determining orbital energies and electronic properties. The eigenvalue theorem in determining ionization potential could be well implemented in the HF method, yet not for the KS-DFT method. However, the KS-DFT calculations at large

basis sets produced ionization potentials closer to the experimental values than the HF method, if calculated using the total energy difference between ionized and non-ionized species.

We also found that the HOMO-LUMO gap in the HF was larger than the gaps obtained from the KS-DFT. Of all performed calculation methods, the B3LYP hybrid functional provided better total energy; and the eigenvalues were located between the HF and the LDA/GGA functionals indicating that the portion of HF exchange in its formulation played a crucial role. At last, this simple comparative performance analysis between the HF and KS-DFT methods hopefully can provide an alternative explanation to address common conceptual difficulties that commonly occur among freshmen studying basic computational chemistry.

SUPPORTING INFORMATION

There is no supporting information of this paper. The data that support the findings of this research are available on request from the corresponding author (YBA).

ACKNOWLEDGEMENTS

YBA thanks to the EMTCCM program and the Department of Chemistry Unhan RI for various supports. NN acknowledges the Australian Research Council and the Center of Exciton Science Australia, Monash University.

CONFLICT OF INTEREST

The authors declare that there are no conflict of interests to disclose.

AUTHOR CONTRIBUTIONS

YBA conducted the computational calculations, wrote, and revised the manuscript; NN wrote and revised the manuscript. The authors agreed to the final version of this manuscript.

REFERENCES

[1] Jones, R. O. 2015. Density functional theory: Its origins, rise to prominence, and future. *Rev. Mod. Phys.* 87(3), 897-923. doi: 10.1103/RevModPhys.87.897

[2] Pribram-Jones, A., Gross, D. A., & Burke, K. 2015. DFT: A theory full of holes?. *Annu. Rev. Phys. Chem.* 66, 283-304. doi: 10.1146/annurev-physchem-040214-121420

[3] Haunschild, R., Barth, A., & Marx, W. 2016. Evolution of DFT studies in view of a scientometric perspective. *J. Cheminform.* 8(52), 1-12. doi: 10.1186/s13321-016-0166-y

[4] Makkar, P., & Ghosh, N. N. 2021. A review on the use of DFT for the prediction of the properties of nanomaterials. *RSC Adv.* 11(45), 27897-27924. doi: 10.1039/D1RA04876G

[5] Nurrosyid, N., Fahri, M., Apriliyanto, Y.B. and Basuki, R., 2022. Novel Absorber Material Design Based on Thiazole Derivatives Using DFT/TD-DFT Calculation Methods for High-Performance Dye Sensitized Solar Cell. *Indones. J. Chem. Stud.* 1(1), 16-23. doi: 10.55749/ijcs.v1i1.5

[6] Apriliyanto, Y.B., Faginas-Lago, N., Evangelisti, S., Bartolomei, M., Leininger, T., Pirani, F., Pacifici, L., and Lombardi, A. 2022. Multilayer Graphtriyne Membranes for Separation and Storage of CO_2: Molecular Dynamics Simulations of Post-Combustion Model Mixtures. *Molecules*. 27(18), 5958. doi: 10.3390/molecules27185958

[7] Faginas-Lago, N., Apriliyanto, Y.B., Lombardi, A. 2020. Carbon capture and separation from CO_2/N_2/H_2O gaseous mixtures in bilayer graphtriyne: a molecular dynamics study. In: Gervasi, O. (ed.) ICCSA 2020. LNCS, vol. 12255, pp. 489–501. Springer, Cham. doi: 10.1007/978-3-030-58820-5_36

[8] Faginas-Lago, N., Apriliyanto, Y.B., Lombardi, A. 2021. Confinement of CO_2 inside carbon nanotubes. *Eur. Phys. J. D* 75(5), 1–10. doi: 10.1140/epjd/s10053-021-00176-7

[9] Jensen, F. 2007. *Introduction to Computational Chemistry*. West Sussex: John Wiley & Sons Ltd.

[10] Cramer C.J. 2004. *Essentials of Computational Chemistry, Theories and Models, Second Edition*. West Sussex: John Wiley & Sons Ltd.

[11] Kim, J., Hong, K., Choi, S., Hwang, S. Y., & Kim, W. Y. 2015. Configuration interaction singles based on the real-space numerical grid method: Kohn–Sham versus Hartree–Fock orbitals. Phys. Chem. Chem. Phys. 17(47), 31434-31443. doi: 10.1039/C5CP00352K

[12] Chakma, U., Ali, M. H., Das, D. K., Boidya, J. R., Khan, M. B. U., Mahmud, M. S., ... & Kumer, A. 2023. First-principles calculations to investigate structural, optical and electronic properties of ZrO_2, $Zr_{0.93}Si_{0.07}O_2$ and $Zr_{0.86}Si_{0.14}O_2$ for dye-sensitised solar cells applications. *Mol. Simul.* 49(15), 1389-1400. doi: 10.1080/08927022.2023.2232887

[13] Neese, F. 2018. Software update: the ORCA program system, version 4.0. *WIREs Comput. Mol. Sci.* 8(1), e1327. doi: 10.1002/wcms.1327

[14] Jmol: an open-source Java viewer for chemical structures in 3D. https://jmol.sourceforge.net

[15] NIST: Atomic Spectra Database - Ionization Energies Form. https://physics.nist.gov/PhysRefData/ASD/ionEnergy.html